Kinetics of furfural aldol condensation with acetone

Korolova, Valeriia; Kikhtyanin, Oleg; Grechman, Evgeniya; Russo, Vincenzo; Wärnå, Johan; Murzin, Dmitry Yu; Kubička, David

Published in:
Catalysis Today

DOI:
10.1016/j.cattod.2023.114272

Published: 01/11/2023

Document Version
Final published version

Catalysis Today 423 (2023) 114272

Contents lists available at ScienceDirect

Catalysis Today

journal homepage: www.elsevier.com/locate/cattod

Kinetics of furfural aldol condensation with acetone

Valeriia Korolova [a], Oleg Kikhtyanin [b], Evgeniya Grechman [a], Vincenzo Russo [c], Johan Wärnå [d], Dmitry Yu. Murzin [d,*], David Kubička [a,b]

[a] Department of Petroleum Technology and Alternative Fuels, University of Chemistry and Technology Prague, Prague, Czech Republic
[b] Technopark Kralupy, University of Chemistry and Technology Prague, Kralupy nad Vltavou, Czech Republic
[c] University of Naples Federico II, Naples, Italy
[d] Åbo Akademi University, Åbo/Turku, Finland

ARTICLE INFO

Keywords:
Furfural
Acetone
Aldol condensation
Kinetic modelling
Thermodynamics

ABSTRACT

Furfural condensation with acetone has been studied over hydrotalcite materials exploring the influence of temperature, furfural to acetone ratio and catalyst loading. Concentration profiles exhibiting limiting conversion values depending on the catalyst amounts along with thermodynamic calculations clearly demonstrating absence of any thermodynamic restrictions point out on catalyst deactivation, which is more pronounced at lower catalyst concentrations. Deactivation is more likely influencing the first step of aldol condensation, rather than subsequent dehydration. A kinetic model has been developed which included catalyst deactivation. Kinetic modelling confirmed an adequate description of the experimental data with the advanced model.

1. Introduction

Today, the development of new technologies to produce motor fuels from alternative sources (in particular, from waste biomass) and to minimize the negative impact of different environmental factors (global warming, climate change, CO_2 release and air pollution) and politico-economic reasons (limited fossil fuel resources, unpredictable prices for conventional hydrocarbons) remains the most important challenge for modern society [1–3]. The conversion of lignocellulose as the component of forestry biomass results in furanic compounds, such as furfural or 5-hydroxymethyl furfural. Both furanics represent high-valued platform molecules that could be easily converted into a range of chemicals by condensation, hydrogenation, oxidation, decarbonylation, etc. [2]. The aldol condensation reaction appears to be one of the most important steps in the conversion of light furanic molecules into fuel-level alkanes after formation of the long-chain carbon precursors followed by their hydrodeoxygenation [4,5]. Usually, aldol condensation reaction is catalyzed by basic homogeneous catalysts, such as the aqueous solutions of NaOH or KOH. However, the use of homogeneous catalysts has a negative impact on the environment, as the amount of wastewater to be cleaned from the hydroxides increases; moreover, it also negatively affects the process economics because of higher production costs [6,7]. Subsequently a substantial effort has been put recently on the development of suitable alternative catalysts, such as heterogeneous basic solids, MgO [8], CaO [9], TiO_2 [10], MgO-ZrO_2 [7,11], alkali-exchanged zeolites [12,13] or heterogeneous acidic solids, ion-exchanged resins [14], zeolites [15], MOFs [16,17], to replace conventional homogeneous catalysts. Among such heterogeneous catalysts, materials derived from layered double hydroxides (LDH), also known as hydrotalcites (HTC), were reported to be promising aldolization catalysts [11,18–25] because of their high activity and a possibility to exploit them at low reaction temperature (20–50 °C). Hydrotalcites can be described by a general formula $[M^{2+}_{1-x}M^{3+}_{x}(OH)_2][A^{n-}_{x/n}\bullet mH_2O]$, where M^{2+} and M^{3+} are divalent and trivalent metal cations, respectively, and A^{n-} is an interlayer anion, typically a carbonate [26,27]. The as-prepared HTCs usually find little application as basic catalysts because they do not possess active sites with the necessary strength. The distinctive feature of the HTC-like materials is their "memory effect", i.e. the ability to restore the original HTC structure upon the calcination of the as-prepared precursor and the interaction of the formed mixed oxide with water [24,28]. As the result of such treatment, meixnerite (magnesium aluminium hydroxide hydrate), i.e. HTC material with interlayer hydroxyls, which are Brønsted-type basic sites, is formed. Consequently, the reconstructed HTCs demonstrate high activity in different catalytic applications that require Brønsted basicity, for example, aldol condensation of furfural and acetone.

Despite many studies covering aldol condensation over heterogeneous catalysts [11,18–25,29,30], only few of them considered the kinetic model of the reaction [11,31–35]. Surprisingly very little

* Corresponding author.
E-mail address: dmurzin@abo.fi (D.Yu. Murzin).

https://doi.org/10.1016/j.cattod.2023.114272
Received 14 April 2023; Received in revised form 5 June 2023; Accepted 18 June 2023
Available online 20 June 2023

Nomenclature

K_j^0	Equilibrium constant at standard conditions for reaction j.
n	Moles, mol.
P	Pressure, bar.
P^0	Standard pressure, bar.
R	Ideal gas constant, J/K/mol.
T	Absolute temperature, K.
T^0	Absolute standard temperature, K.

Greek symbols

ΔG_f^0	Gibbs free energy of formation at standard conditions, J/mol.
ΔG_r^0	Gibbs free energy of reaction at standard conditions, J/mol.
$\Delta G_{r,j}^{\Phi}$	Gibbs free energy of reaction at 1 bar and chosen temperature, J/mol.
ΔH_f^0	Enthalpy of formation at standard conditions, J/mol.
ΔH_r^0	Enthalpy of reaction at standard conditions, J/mol.
$\nu_{i,j}$	Stoichiometric matrix composed by i components and j reactions, -

information is available related to reaction kinetics, including kinetic regularities (e.g. reaction order in substrates) and modelling of concentration behavior across a broad range of parameters (temperature, ratio between parameters, catalyst loading, etc.). Moreover, the published kinetic studies did not consider the contribution of a catalyst's deactivation during aldol condensation reaction. In general, several different deactivation causes were described in literature: the fouling of the catalyst surface with high molecular weight products formed by consecutive aldol condensation steps, leaching of metals from the catalyst in the aqueous medium, and the occurrence of Cannizzaro reaction [11,36–40]. Nevertheless, the deactivation factor was not considered when compiling mathematical models of aldol condensation. This work was subsequently initiated to fill such apparent void and has the objective to investigate the concentration profiles of the reactants and products upon changing the catalyst concentration, temperature, furfural to acetone molar ratio as well as considering the effect of Cannizzaro reaction on the overall kinetics of the reaction.

2. Experimental

2.1. Catalyst preparation and thermal treatment

The MgAl hydrotalcite (HTC) materials with the molar ratio Mg/Al= 3 were prepared using a conventional co-precipitation method described elsewhere [19,41]. For the preparation of a salt solution, $Mg(NO_3)_2{\cdot}6\ H_2O$ (99.9%, Lach:Ner, Neratovice, Czech Republic) and $Al(NO)_3{\cdot}9\ H_2O$ (98.8%, Lach:Ner, Czech Republic) were used, while NaOH (99.6%, Lach:Ner, Czech Republic) and Na_2CO_3 (99%, Penta, Czech Republic) were applied in the case of an alkaline solution. The aqueous salt solution (total metal ion concentration of 0.5 mol·l^{-1}) and the aqueous alkaline solution of Na_2CO_3 (0.2 mol·l^{-1}) and NaOH (1 mol·l^{-1}) were added at the same time to 200 ml of distilled water. The co-precipitation of the two solutions was performed at 25 °C, and the pH value of the reaction mixture was kept constant at pH= 10 by adjusting the flow rate of the added alkaline solution. The co-precipitation was carried out for 3 h at the constant stirring rate of 420 rpm. Thereafter, the obtained precipitate was aged at 25 °C for 1.5 h under stirring conditions, followed by filtration and washing with distilled water and drying first for 12 h at room temperature and then for 12 h at 60 °C. The thermal treatment of the as-prepared HTC was carried out in a muffle oven at 450 °C in static air for 3 h giving MgAl mixed oxides. After calcination, the prepared mixed oxides were stored in a desiccator to prevent their contact with atmospheric CO_2. The rehydration strategy of the mixed oxides was adopted from our previous studies [22,23]. It was performed by the contact of the calcined solids with 23 g of distilled water under static conditions in a closed small bottle for 20 min at 30 °C to totally exclude the impact of the environment on the rehydration procedure. The resulting catalysts were separated from an aqueous phase by filtration with a Buchner funnel and a vacuum pump. The rehydrated samples were immediately transferred to a reactor loaded with furfural and acetone to initiate the aldol condensation reaction.

2.2. Physico-chemical characterization

The phase composition of the as-prepared MgAl HTC, calcined mixed oxide, reconstructed HTC and spent catalysts was determined by X-Ray diffraction using a diffractometer PANanalytical X'Pert3 Powder and CuKα radiation. The chemical composition of the samples was analyzed by AAS using Agilent 280 FS AA spectrometer. The absence of Mg or Al leaching into the reaction products of aldol condensation was confirmed by ICP analysis using Agilent 5100 ICP OES. The textural properties of the as-prepared, calcined and rehydrated samples were determined by N_2 physisorption using a static volumetric adsorption system (TriFlex analyzer, Micromeritics). The thermal analysis of the as-prepared and rehydrated HTC samples in N_2 atmosphere was performed using Labsys EVO TG-DTA/DSC instrument. The spent catalysts after reaction were also analyzed on the same unit in O_2 atmosphere.

2.3. Catalytic tests

Acetone (99.9%, Penta, Czech Republic) and furfural (99%, Sigma-Aldrich, USA) were used as reactants in all catalytic experiments. First, the received furfural was distilled using a rotary evaporator and then stabilized with 2,6-di-tert-butyl-4-methylphenol (DBMP, 99%, Sigma-Aldrich, USA) and stored in a cold place, to prevent the re-oxidation of the freshly distilled furfural and to increase the reproducibility of catalytic results, as described in detail in [21]. The aldol condensation reaction of furfural with acetone was carried out in a 250 ml stirred glass batch reactor during 3 h at various reaction temperatures (10–50 °C), ambient pressure and stirring rate 420 RPM. A reaction temperature of 10 °C was obtained by immersing the flask with the solution in an ice bath with occasional additions of ice to maintain a constant temperature. A different amount (0.15/0.29/0.44/0.58 g) of a freshly calcined mixed oxide was taken in the experiments for a rehydration step resulting in rehydrated MgAl HTC, denoted further as a catalyst, with a mass of 0.25/0.50/.75/1.00 g, respectively. The reaction mixture consisted of furfural, acetone (molar ratios F:Ac =1:3/5/10/20 with the same amount of furfural equal to 12.43 g) and a rehydrated catalyst. As described previously [19,22,23], the absence of both external and internal mass transfer effects was confirmed by performing catalytic experiments with changing stirring rate and catalyst particle size. Samples were periodically taken from the reactor at regular intervals, filtered form the catalyst, diluted with methanol (1:20 by volume) and analyzed by Agilent 7890 A gas chromatograph equipped with the flame ionization detector (FID) using an HP 5 capillary column (30 m/0.32 mm ID/0.25 μm). Selected liquid samples were additionally analyzed by GC-MS using GC-MS Agilent 7010 to identify reaction products.

Catalytic results on aldol condensation of furfural with acetone were quantified with commercially available compounds (4-(2-Furyl)− 3-buten-2-one, Alfa Aesar, 98%) as well as using conventional internal standard methods and described by conversion and selectivity parameters that were calculated as follows:

$$\text{Furfural conversion (t) (mol\%)} = 100 \times (\text{moles of furfural}_{t=0} - \text{moles of furfural}_{t=t})/\text{moles of furfural}_{t=0} \quad (1)$$

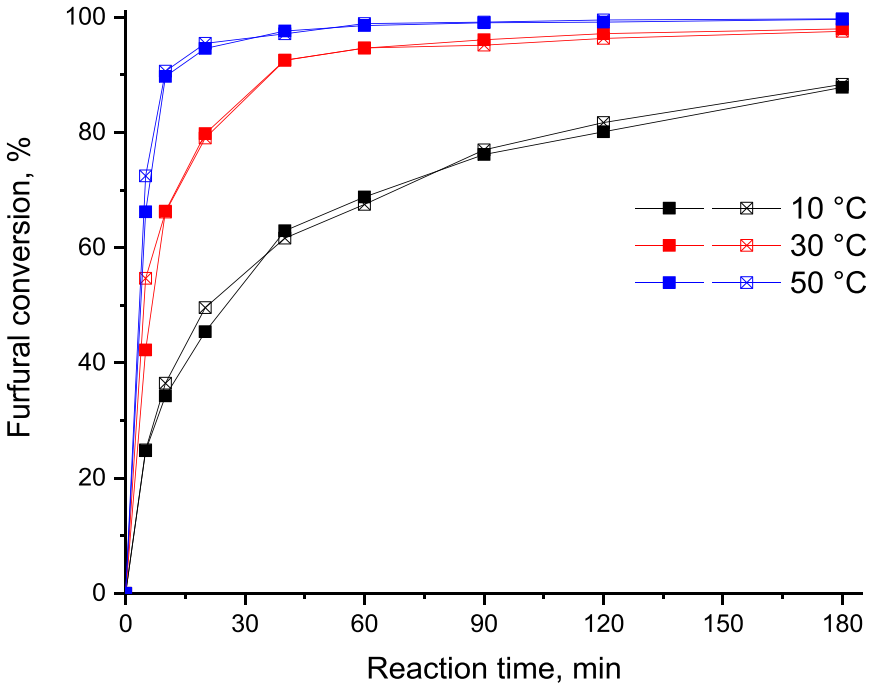

Fig. 1. Dependence of furfural conversion on reaction time in the aldol condensation of furfural with acetone over rehydrated MgAl HTC. Conditions: $m_{(cat)}$= 1.00 g, molar ratio F:Ac= 1:5. Hollow and filled squares stand for repeated experiments.

where t stands for reaction time.

Selectivity to product *i* (mol%)=100×(mole of reactant converted to product i) / (total converted moles) (2)

Carbon balance was monitored in all experiments as the total number of carbon atoms detected in each organic compound with C_n atoms (where n = 3, 5, 8, …, etc.) divided by the initial number of carbon atoms in F + Ac feed:

Carbon balance (%) = (3 mol C_3 + 5 mol C_5 …+ nmol C_n) /(3 mol $C_{3(t=0)}$ + 5 mol $C_{5(t=0)}$) (3)

Based on the calculations, the carbon balance was above 95% in all performed experiments.

In selected cases, experiments were repeated 2–3 times to confirm reproducibility of the catalytic results.

Acetone self-condensation was evaluated in separate experiments at the same conditions used for aldol condensation of furfural and acetone. It yields of acetone self-condensation products below 2–3% even at the highest reaction temperature, and thus it was excluded from further consideration.

3. Results and discussion

3.1. Physico-chemical characterization

The XRD pattern of the as-prepared MgAl HTC evidenced the phase purity and high crystallinity of this material. The calcination of the precursor at T = 450 °C produced MgAl mixed oxide with periclase structure. The rehydration of the mixed oxide in static conditions resulted in the recovery of the HTC structure, as evidenced by the presence of intensive characteristic reflections in the XRD pattern of the rehydrated sample. The obtained results agreed well with those obtained in our previous studies for similar MgAl HTC materials [19,22,23] and confirmed the effectiveness of the used "static" rehydration method.

The properties of the as-prepared HTC precursor, mixed oxide and rehydrated HTC sample were also characterized by N_2 physisorption. The results obtained from these methods were also very close to those obtained for similar materials in our previous studies [19,22,23].

TGA results for the as-prepared HTC precursor, mixed oxide and rehydrated HTC also corresponded to those obtained previously for similar materials and confirmed the quality of materials used in the present study.

3.2. Catalytic data

Based on approach developed in our previous studies [20,22], several experiments were initially performed to evaluate the possibility of leaching, i.e. the partial dissolution of a rehydrated HTC catalyst in a reaction mixture. Experiments with the separation of the catalyst from a reaction mixture and Mg/Al determination in solid and liquid phases proved the absence of the leaching effect.

3.2.1. Influence of reaction temperature

The influence of reaction temperature on the catalytic performance of rehydrated MgAl HTC was studied at three different temperatures – 10, 30 and 50 °C. Fig. 1 represents a change in furfural conversion with the reaction time in experiments with 1.00 g of catalyst.

After 180 min of the reaction, a very high furfural conversion was observed (>88%) for all examined temperatures that correlates well with the previous studies [6,19,23]. The lowest conversion of 88% was observed as expected at 10 °C, while an increase in reaction temperature from 10° to 50°C resulted only in a slight increase in a final furfural conversion from 88% to 99%. At the same time Fig. 1 clearly confirms that elevation of the reaction temperature increased the rate as could be seen for example through differences in furfural conversion after 5–30 min

Because the reaction thermodynamics is favorable for aldol condensation, as will be discussed below, it is not surprising that furfural conversion after 180 min of the reaction differs only slightly depending on the reaction temperature. It is, however, interesting that there were substantial changes in selectivity at the same conversion level, implying that the rates of chemical reactions comprising the reaction network (e. g. formation of 4-(2-furyl)– 4-hydroxybutan-2-one, FAc-OH, through

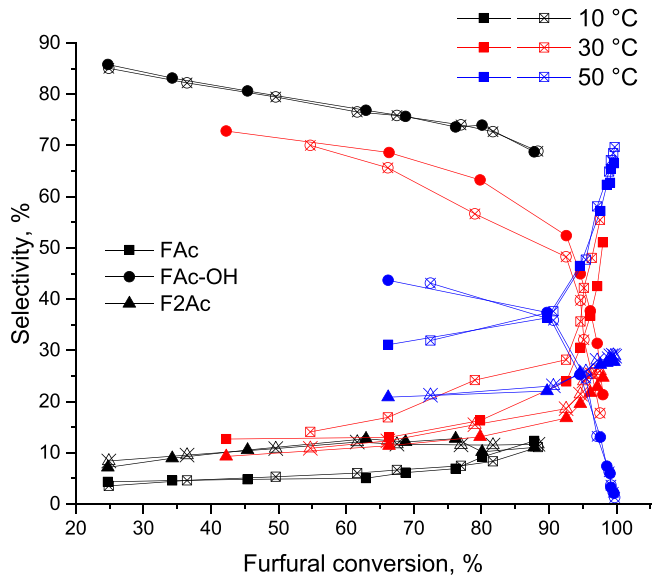

Fig. 2. Dependence of selectivity to the main reaction products on furfural conversion in the aldol condensation of furfural with acetone over the rehydrated MgAl HTC. Conditions: $m_{(cat)}$= 1.00 g, molar ratio F:Ac= 1:5.

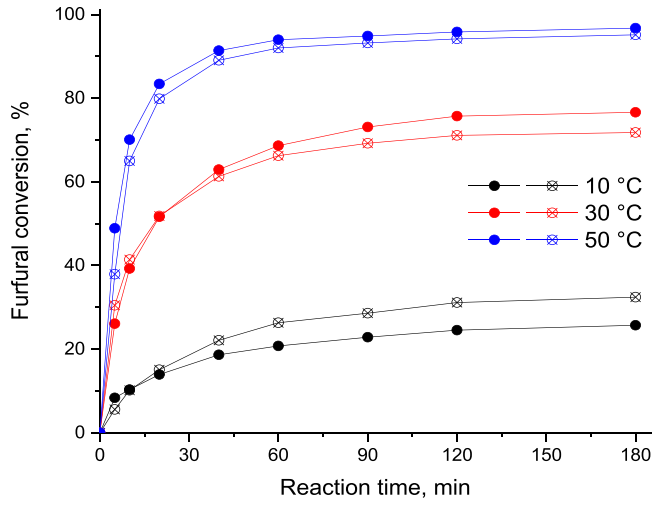

Fig. 3. Dependence of furfural conversion on reaction time in the aldol condensation of furfural with acetone over rehydrated MgAl HTC. Conditions: $m_{(cat)}$= 0.50 g, molar ratio F:Ac= 1:5.

addition of furfural to acetone; subsequent dehydration to 4-(2-furyl)−3-buten-2-one, FAc, and finally addition of the second furfural molecule giving F_2Ac) have different activation energies. To illustrate this point, data at isoconversion of 88% can be considered. At 10 °C, FAc-OH is the main reaction product (Fig. 2) with a selectivity of 69%, followed by FAc (12%) and F_2Ac (12%). An increase in the reaction temperature to 30 °C leads to intensive dehydration with formation of FAc (26%) and F_2Ac (18%), while selectivity to FAc-OH decreases to 50%. A further increase in the reaction temperature to 50 °C results in formation of FAc as the main reaction product with selectivity of 37%, followed by FAc-OH (36%) and F_2Ac (23%).

Small differences in the values of initial conversion with 1.00 g catalyst prompted evaluation of the temperature influence with a lower catalyst loading of 0.50 g (Fig. 3).

From Fig. 3 it is evident that the reaction temperature has a significant effect on the aldol condensation in terms of reactivity and also catalyst deactivation. An increase in the reaction temperature resulted in

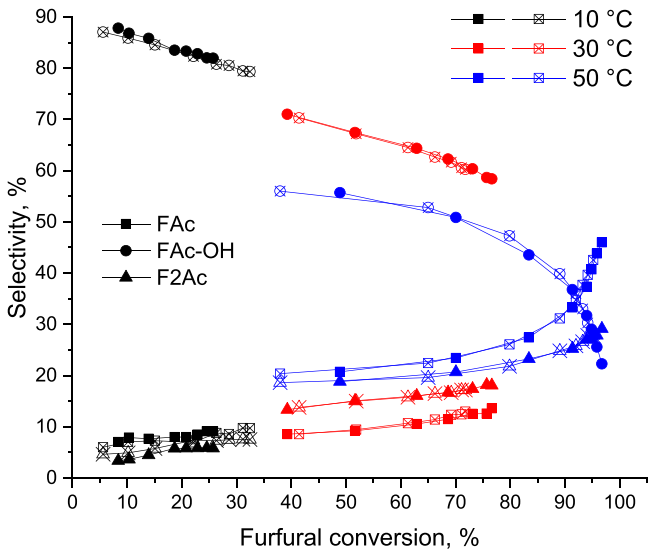

Fig. 4. Dependence of selectivity on furfural conversion over rehydrated MgAl HTC. Conditions: $m_{(cat)}$= 0.50 g, molar ratio F:Ac= 1:5.

elevation of furfural conversion. At the same time, as mentioned above, the aldol condensation with furfural is not limited by thermodynamics, therefore incomplete conversion levelling off at prolonged reaction time of 3 h can be attributed to catalyst deactivation. The lowest furfural conversion of 29% was observed at 10 °C after 180 min, with the corresponding levels at 30 °C and 50 °C being 74% and 96% respectively.

While there are some minor differences in the absolute values of selectivity for two catalyst loadings, the trends of selectivity dependence on conversion for a lower catalyst loading (Fig. 4) were similar to the ones observed for the experiments with twofold higher amounts. Namely, an increase in reaction temperature is beneficial for dehydration of FAc-OH, formation of FAc and occurrence of the second condensation step giving F_2Ac. At 10 and 30 °C, FAc-OH was the main reaction product with selectivity of 76 (extrapolated to 40% conversion) and 70% at 40% conversion, respectively. It was followed by FAc (11% and 9%, respectively) and F_2Ac (9% and 13%, respectively) at the furfural conversion of 40% (again selectivity at 10 °C was calculated by extrapolating the selectivity trends to 40% furfural conversion to allow isoconversion data comparison). At 50 °C, FAc-OH is still prevailed decreasing rather rapidly after 70% conversion and beyond ca. 90% conversion the most dominant product was FAc.

3.2.2. *Influence of F/Ac ratio*

The effect of F/Ac molar ratio on the catalytic performance of rehydrated MgAl HTC was studied under four different ratios: 1:3, 1:5, 1:10, 1:20. Fig. 5A represents the dependence of furfural conversion on the reaction time at catalyst loading m= 1.00 g and reaction temperature of 30 °C.

As in the experiments carried out under various temperatures with the same catalyst amount, very high furfural conversion was observed (96–99%) for all tested F/Ac ratios after 180 min. Furthermore, conversion close to 90% (87–99%) was achieved already after 1 h. By comparing furfural conversion at 10 min of the reaction it can be unequivocally concluded that an increase in the amount of acetone in the reaction mixture positively influenced furfural conversion with the lowest value of 54% observed for the molar ratio F/Ac= 1:3. An increase in the amount of acetone elevated conversion level to 66% and 81% for respectively F/Ac= 1:5 and 1:10 ratios. The maximum furfural conversion of 90% after 10 min was obtained for the highest tested F/Ac molar ratio of 1:20.

In general, such kinetic dependences can be related to an increase in the reaction rate at higher acetone concentrations. On the other hand, a

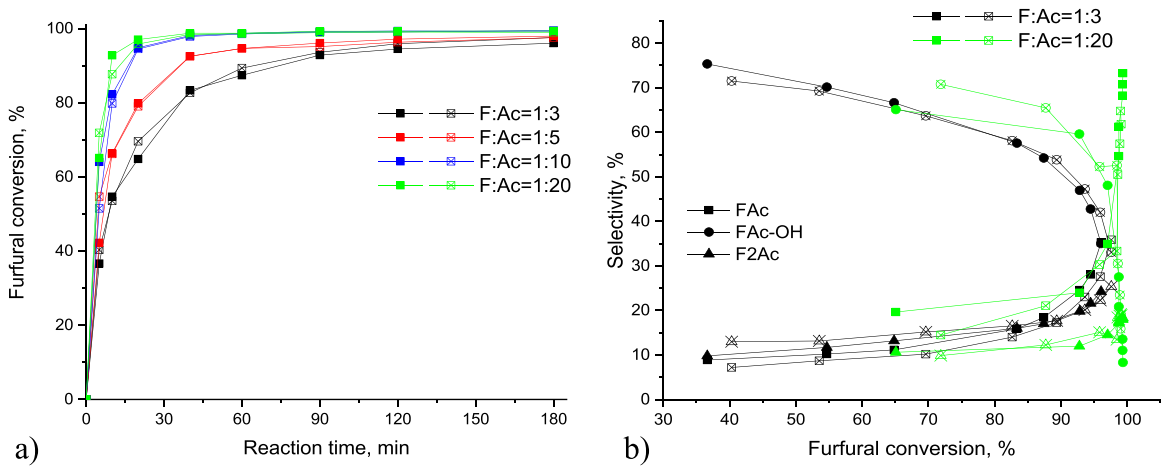

Fig. 5. Dependence of a) furfural conversion on reaction time over rehydrated MgAl HTCs and b) product selectivity on furfural conversion in aldol condensation of furfural with acetone. Conditions: $m_{(cat)}$= 1.00 g, reaction temperature 30 °C.

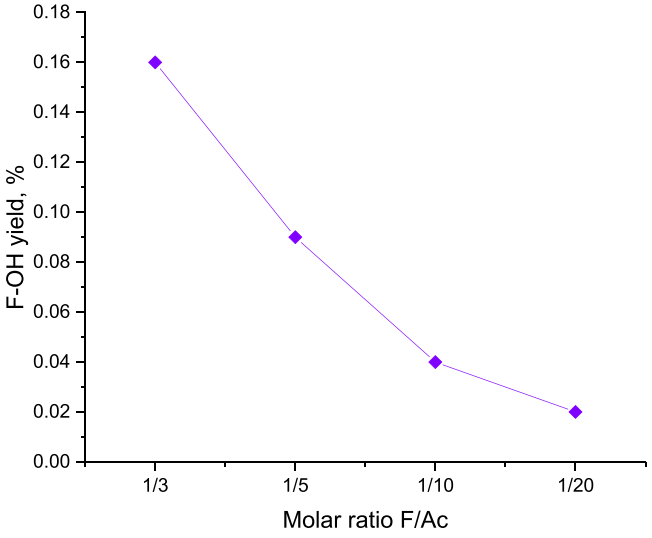

Fig. 6. Dependence of the furfuryl alcohol yield on F/Ac molar ratio. Conditions: $m_{(cat)}$= 1.00 g, reaction temperature 30 °C, $t_{reaction}$= 10 min.

high excess of one compound typically leads to zero order kinetics in this compound as can be clearly seen for the data at F:Ac ratios of 10 and 20. An alternative explanation involves the occurrence of the Cannizzaro reaction with the formation of both furfuryl alcohol (F-OH) and furoic acid (F-OOH) as a parallel route during the base-catalyzed aldol condensation reaction at high furfural concentrations in the reaction mixture. Generally, both furfural and acetone could compete for the same active sites on the surface of a basic catalyst [36]. The abstraction of α-proton in acetone molecule results in the formation of the enol, a key intermediate in the aldol condensation [11,25]. Alternatively, interactions of furfural with a basic site initiate the Cannizzaro reaction. Both the aldol condensation and the Cannizzaro reaction occur on the same active sites, therefore, deactivation and poisoning of a basic catalyst with furoic acid formed by the Cannizzaro reaction should affect the outcome of the aldol condensation. Formation of F-OH as a product was detected by GC analysis in all experiments, moreover, its yield after 10 min decreases from 0.16% to 0.02% with the increase in the acetone amount in the reaction mixture from F/Ac= 1:3–1:20, respectively (Fig. 6). F-OOH formation was not detected by GC, indicating that, once formed, it readily reacts with the basic sites of a catalyst and forms surface furoate species, as described in [25,36].

The increase in the acetone amount in the reaction mixture also slightly affected product selectivity at $T_{reac.}$ = 30 °C (Fig. 5B). The

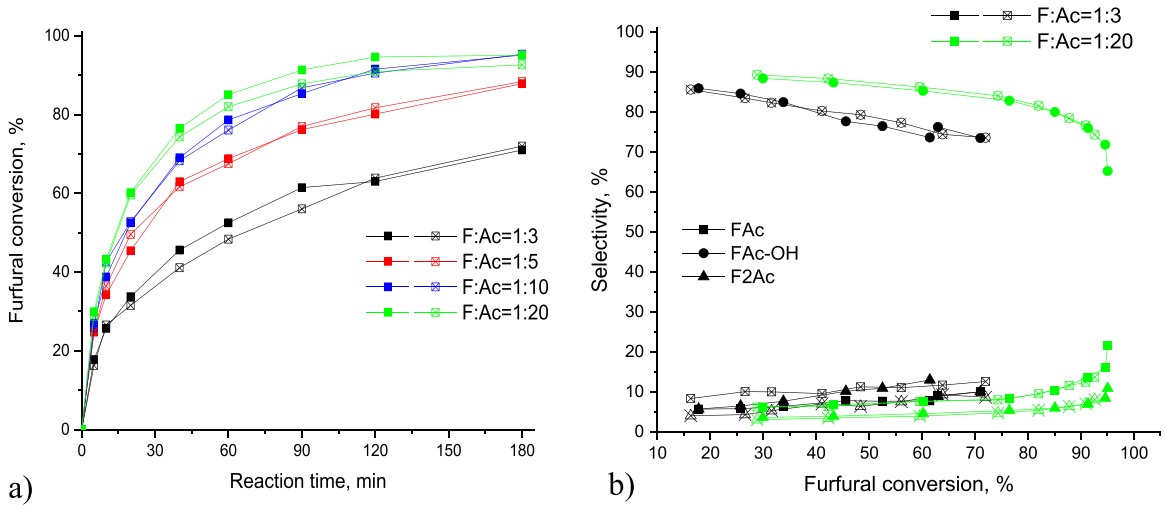

Fig. 7. Dependence of a) furfural conversion on the reaction time and b) selectivity on furfural conversion for the rehydrated MgAl HTCs in the aldol condensation of furfural with acetone. Conditions: $m_{(cat)}$= 1.00 g, $T_{reaction}$= 10 °C.

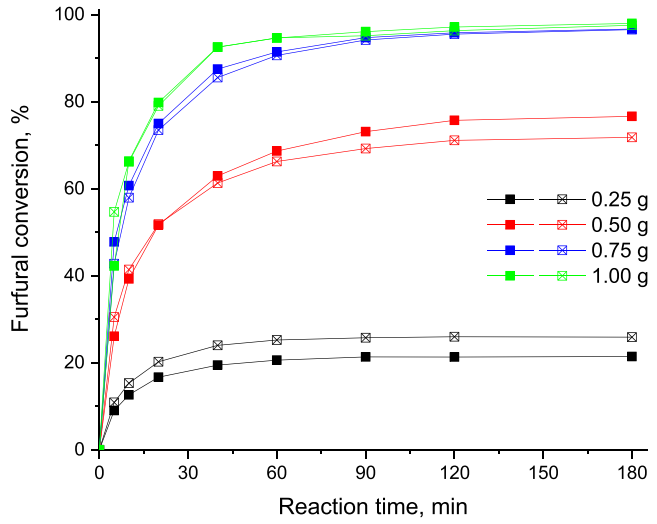

Fig. 8. Dependence of furfural conversion on reaction time over rehydrated MgAl HTCs in the aldol condensation of furfural with acetone using various catalyst loading. Conditions: F/Ac= 1:5, reaction temperature 30 °C.

influence of F/Ac molar ratio on the performance of rehydrate hydrotalcites at 10 °C was also investigated (Fig. 7a).

Although an increase in furfural conversion is slower if compared with experiments at 30 °C, a general trend is similar: furfural conversion increases with increasing acetone amount in a reaction mixture. The lowest furfural conversion of 71% after 180 min was observed for F: Ac= 1:3. An increase in acetone amount leads to an increase in furfural conversion to 88–95%. The Cannizzaro reaction also takes place under these reaction conditions: F-OH is detected by GC in all reaction products. Similar to experiments described above, a decrease in F-OH yield after 10 min of reaction from 0.14% to 0.04% was observed with an increase in the amount of acetone in the reaction in the molar ratios F/Ac= 1:3 and 1:20, respectively. At these reaction conditions, selectivity (Fig. 7B) was also influenced by changes in the amount of acetone. For all experiments, FAc-OH was the main reaction product and its selectivity slightly increased with an increase in the acetone amount from 74% to 83%. A minor decrease in selectivity of both dehydrated FAc and F_2Ac products was observed with an increase in acetone amount.

3.2.3. *Influence of the catalyst loading*

The influence of the catalyst amount on aldol condensation of furfural with acetone was investigated using four different catalyst loadings of freshly calcined and subsequently rehydrated HTC. Fig. 8 illustrates dependence of furfural conversion on the reaction time, using various amounts of catalyst. From Fig. 8, it is obvious that the increase of the catalyst weight leads to increased furfural conversion. The lowest conversion of 24% after 3 h was observed using 0.25 g of catalyst. An additional increase in the catalyst weight to 0.50 g led to a three-fold increase in the final conversion to 67%. Experiments with 0.75 g and 1.00 g of catalyst resulted in furfural conversion– of 97% and 98% after 3 h, respectively. Furthermore, for both these catalyst loadings, furfural conversion above 90% was obtained just after 60 min (Fig. 8).

Data in Fig. 8 along with thermodynamic calculations to be presented in the subsequent section indicate that aldol condensation is not limited by thermodynamics, as the latter is not depending on the catalyst loading. Moreover, calculations of the Gibbs energy (see below) unequivocally confirm absence of any thermodynamic restrictions. Subsequently, such behavior as observed in Fig. 8 can be ascribed to catalyst deactivation, which is more profound at lower catalyst concentrations as can be expected.

In description of catalyst deactivation kinetics, often selectivity is treated separately from activity assuming that a part of the catalyst surface is progressively covered by coke, while the relative ratio of surface coverages for various species remains the same. Subsequently selectivity also does not change even if the level of deactivation is different. To clarify if such assumption can be used for modeling of kinetic data in the current case it was instructive to explore if the catalyst loading influences selectivity vs conversion profiles (Fig. 9).

As can be seen in Fig. 9a, there are minor changes in selectivity vs conversion at different catalyst amounts and almost the same yields are obtained up to the conversion level of ca. 70% (Fig. 9b). Some differences could be seen at higher conversions, as higher yields of FAc-OH were observed at higher catalyst loading, which might mean that deactivation is more likely influencing the first step of aldol condensation – the formation of FAc-OH, rather than the subsequent dehydration. This can be also seen through changes in the product distribution at close to complete conversion levels for catalyst loading of 0.75 g and 1.00 g, namely FAc became the main reaction product with yields 35% and 52%, respectively.

3.3. *The properties of catalysts after reaction*

Spent samples after catalytic experiments were characterized by XRD, and obtained results are presented in the SI. All spent catalysts from experiments with 0.5 g and T = 10, 30 and 50 ° possessed HTC

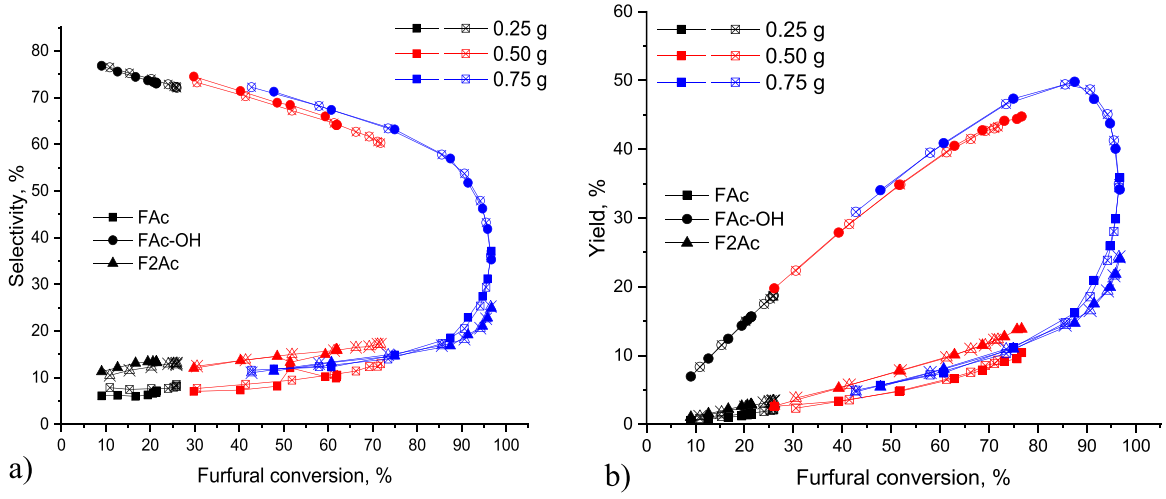

Fig. 9. Dependence of a) selectivity and b) yield of the main reaction products on furfural conversion observed over rehydrated MgAl HTCs in the aldol condensation of furfural with acetone using various catalyst loading. Conditions: F/Ac= 1:5, reaction temperature 30 °C.

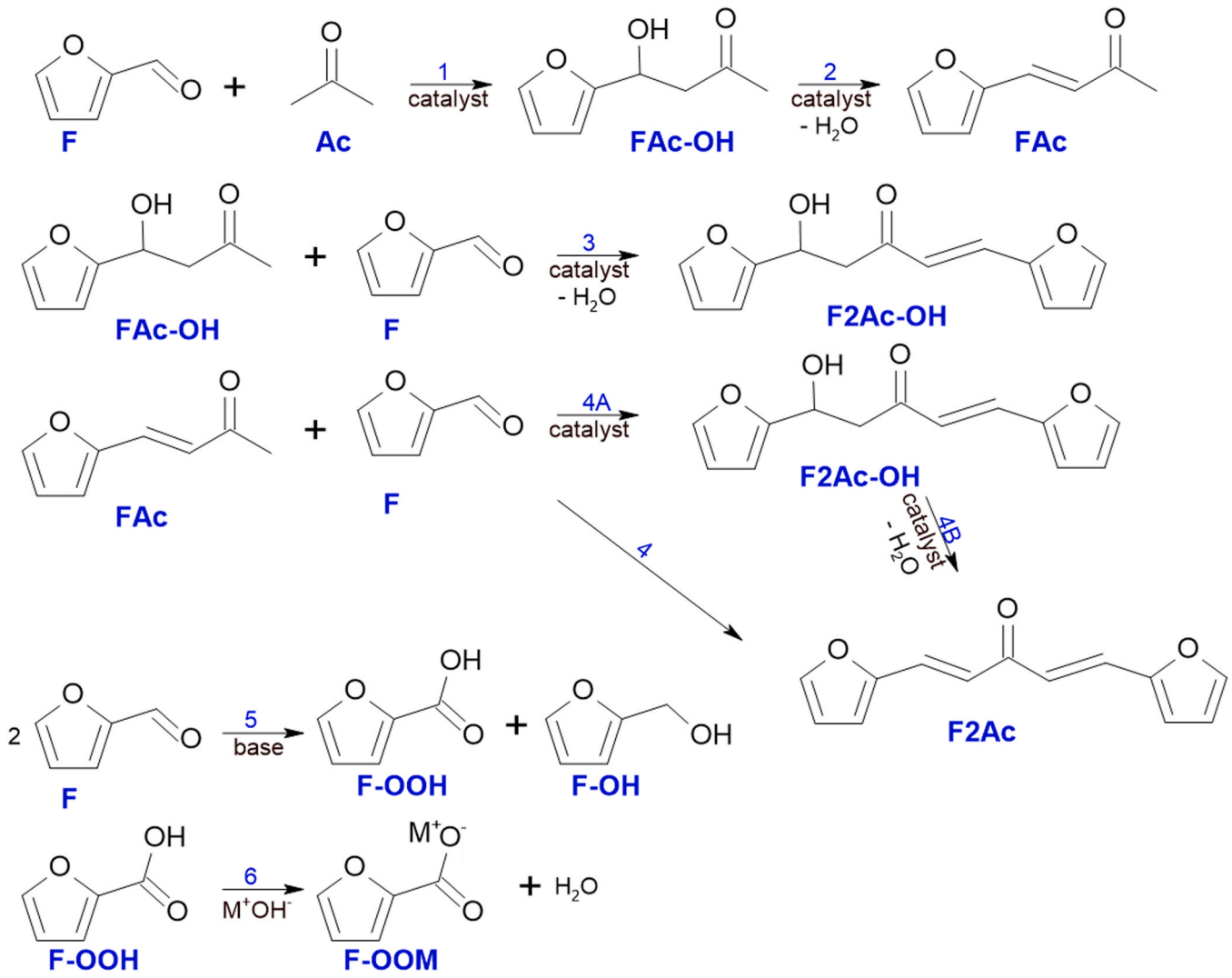

Fig. 10. Reaction network of aldol condensation of furfural with acetone. *F- furfural, Ac-acetone, FAc-OH- 4-(furan-2-yl)– 4-hydroxybutan-2-one, FAc - 4-(furan-2-yl) but-3-en-2-one, F2Ac- 1,5-di(furan-2-yl)penta-1,4-dien-3-one, F2Ac-(OH)- 1,5-di(furan-2-yl)– 5-hydroxypent-1-en-3-one, F-OH- furfuryl alcohol, F-OOH- furoic acid, F-OOM- a salt of furoic acid.*

structure without any presence of reflections from other phases. Nevertheless, characteristic HTC reflections slightly increased in intensity with the growth of reaction temperature. The gradual degradation of HTC structure was also detected in samples after experiments with decreasing catalysts weight. If only 0.25 g of MgAl sample was used for catalytic experiment, the XRD pattern of the spent catalyst evidenced the appearance of reflections from MgO. The obtained XRD results agreed with observed trends in furfural conversion for corresponding catalytic experiments (see Figs. 3 and 8). It could be therefore assumed that the stability of HTC framework during catalytic experiments correlated with the amount of unreacted furfural in a reaction mixture, i.e. presumably also with the occurrence of Cannizzaro reaction discussed above. Definitely, the detailed analysis of the impact of reaction conditions on the HTC crystalline structure of rehydrated samples is a topic for an additional investigation, and this is outside the scope of the present study.

Spent samples after catalytic experiments with different catalyst loading were also studied by TGA. The weight loss of the spent samples slightly increased with decreasing the amount of a catalyst taken for the experiments. Fig. 8 demonstrates that the decrease of the catalyst loading led to a decline in furfural conversion. Therefore, the observed trend in the weight loss for spent catalysts according to TGA study allowed suggesting that non-desorbed species in the spent samples could be formed as the consequence of the contact of catalysts with excessive furfural in a reaction mixture, i.e. because of the occurrence of Cannizzaro reaction, rather than by consecutive condensation steps. The consideration of DTG profiles also confirmed this suggestion: as compared to results for both as-prepared and rehydrated HTCs, the characteristic peak at ≈ 400 °C in the DTG profiles of spent catalysts was noticeably broader with a definite shoulder appearing in a low-temperature region. Previously, it was shown [36] that the formation of surface furoate species in spent catalysts as the consequence of Cannizzaro reaction during aldol condensation was characterized by the appearance of an additional peak in the DTG profiles at around 350 °C. Taken together, the results of TGA studies led to the conclusion that the deactivation of catalysts observed in the catalytic experiments of the present study was mostly concerned with the occurrence of Cannizzaro reaction.

3.4. Analysis of thermodynamics

Enthalpy (ΔH_r^0) and Gibbs free energy (ΔG_r^0) at standard conditions were calculated by following the thermodynamic approach [42], starting from the standard enthalpy (ΔH_f^0) and Gibbs free energy (ΔG_f^0) of formation from the elements retrieved from CHEMCAD database [43, 44] using the Joback approach [45–47], as illustrated below

Table 1
Enthalpy and Gibbs free energy formation for each component (*i*) and stoichiometric matrix for component *i* for reaction *j*.

Component	ΔH_f^0 [kJ/mol]	ΔG_f^0 [kJ/mol]	i/j	1	2	3	4	5
F	-147.85	-57.12	1	-1	0	-1	-1	-2
Ac	-1821.40	-153.20	2	-1	0	0	0	0
FAc-OH	-381.29	-200.52	3	+1	-1	-1	0	0
H_2O	-241.83	-228.44	4	0	+1	0	+1	0
FAc	-178.32	-55.50	5	0	+1	0	-1	0
F2Ac	-138.81	43.54	6	0	0	0	+1	0
F2Ac-(OH)	-390.89	-134.42	7	0	0	+1	0	0
F-OH	-201.51	-94.42	**8**	0	0	0	0	+1
F-OOH	-399.55	-301.51	**9**	0	0	0	0	+1

*F- furfural, Ac-acetone, FAc-OH- 4-(furan-2-yl)– 4-hydroxybutan-2-one, FAc - 4-(furan-2-yl)but-3-en-2-one, F2Ac- 1,5-di(furan-2-yl)penta-1,4-dien-3-one, F2Ac-(OH)- 1,5-di(furan-2-yl)– 5-hydroxypent-1-en-3-one, F-OH- furfuryl alcohol, F-OOH- furoic acid.

Table 2
Enthalpy and Gibbs free energy at standard conditions, equilibrium constants at standard conditions (K_j^0).

ΔH_r^0 [kJ/mol]	ΔG_r^0 [kJ/mol]	K_j^0
1.59 10^3	9.80	1.92 10^{-2}
-38.9	-83.4	4.12 10^{14}
138	123	2.59 10^{-22}
-54.5	-72.3	4.60 10^{12}
-305	-282	2.24 10^{49}

$$\Delta H_{r,j}^0 = \sum_j \nu_{i,j} \cdot \Delta H_{f,i}^0 \tag{4}$$

$$\Delta G_{r,j}^0 = \sum_j \nu_{i,j} \cdot \Delta G_{f,i}^0 \tag{5}$$

The equilibrium constant of each reaction was calculated from its dependence on the Gibbs energy

$$K_j^0 = \exp\left(-\frac{\Delta G_{r,i}^0}{RT}\right) \tag{6}$$

The dependence of the reaction free Gibbs energy with temperature was included by implementing the Gibbs-Helmholtz equation valid at $P = 1$ bar ($\Delta G_{r,j}^{\Phi}$)

$$\frac{\Delta G_{r,j}^{\varphi}(T)}{T} = \frac{\Delta G_{r,j}^0}{T^0} + \Delta H_{r,j}^0 \left(\frac{1}{T} - \frac{1}{T^0}\right) \tag{7}$$

The calculated enthalpy and Gibbs free energy formation for each component (*i*) present in the reaction network (Fig. 10) are reported in Table 1.

Starting from these values, the enthalpy and Gibbs free energy for each reaction (*j*) at standard conditions, equilibrium constants at standard conditions (K_j^0), enthalpy and Gibbs free energy at different temperatures and pressure were calculated. For calculations, the lumped reaction of 4 A and 4B was considered, giving directly F_2A_C from FAc and furfural.

A temperature range was investigated (T_{min}=323 K, T_{max}=423 K). The results of the calculations reported in Table 2 and Fig. 11, reveal that the reaction 3 is not spontaneous, as could be also seen from the experimental data as well. All the other reactions are spontaneous with the lowest ΔG_r exhibited by reaction 2.

3.5. Kinetic modelling

For kinetic modelling, the reaction network presented in Fig. 10 was adopted. As the reaction 3 was considered to be thermodynamically not feasible, it was not included in the modelling. Adsorption of all reactants on the surface of the catalysts was supposed to be feasible giving the following rate expressions:

$$\begin{aligned} r_1 &= \frac{k_1 c_F c_{Ac}}{D^2}; \\ r_2 &= \frac{k_2 \quad c_{FAcOH}}{D}; \\ r_{4A} &= k_{4A} \frac{c_{FAc} c_F}{D^2}; \\ r_{4B} &= k_{4B} \frac{c_{F2AcOH}}{D}; \\ r_5 &= k_5 c_F^2; \\ r_6 &= k_6 c_{FCOOH} \end{aligned} \tag{8}$$

where

$$D = 1.0 + K_F \quad c_F + K_{Ac} \quad c_{Ac} + K_{FAC} \quad c_{FAc} + K_{F2AcOH} \quad c_{F2AcOH} + K_{F2Ac} \quad c_{F2Ac} + K_{FOH} \quad c_{FOH} \tag{9}$$

As follows from Eq. (8) reactions 5 and 6 were considered to be non-heterogeneous catalytic, thus they do not contain the denominator (Eq. (9)).

The generation equations for the reactants can be easily written from Fig. 10, as exemplified below for furfural:

$$-\frac{dC_{furfural}}{dt} = \rho_B \left(r_1 + r_{4A} + 2r_5\right) a \tag{10}$$

Where r_i are the rates of the corresponding reactions, ρ_B is the catalyst bulk density (m_{cat}/V_L),.

and a is the activity function.

The parameter estimation was carried out with a software ModEst [47] using as the objective function the squared difference between all experimental and calculated values combined, which was minimized by using hybrid simplex and Levenberg-Marquardt algorithms. The rate constants were calculated using the modified Arrhenius equation with the pre-exponential factor corresponding to the rate constant at the average temperature,

$$k = k_0 e^{\frac{-Ea}{R}\left(\frac{1}{T} - \frac{1}{T_{avg}}\right)} \tag{11}$$

which was 303 K in the current case.

Several empirical and semi-empirical activity functions were tested, reflecting deactivation by carbon deposition on the catalyst surface. Finally, the expression for the activity coefficient was adopted, which

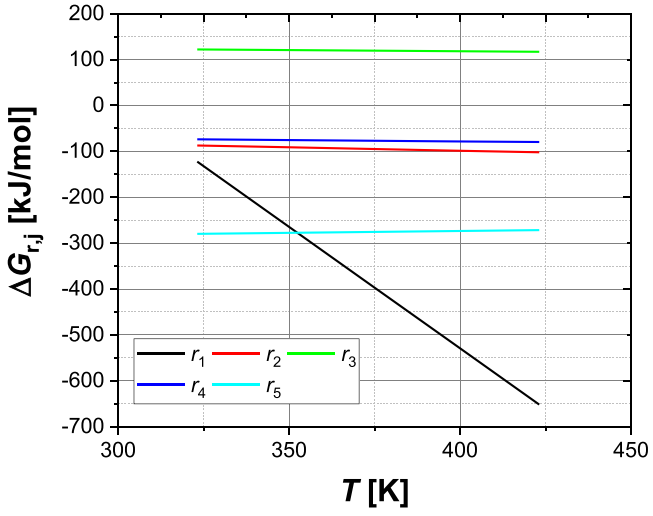

Fig. 11. Gibbs free energy as a function of temperature for different reactions in Fig. 10.

Table 3
Values for kinetic parameters and statistical analysis.

Parameter	Value	Units	Standard error (%)
k_1/K_F^2	0.00022	$(dm^3)^2/mol/g/min$	6.1
k_2/K_F	0.0013	g/dm3/min	8.2
k_{4A}/K_F^2	0.0062	$(dm^3)^2/mol/g/min$	7.3
k_{4B}/K_F	0.0063	g/dm3/min	11.6
k_5	$0.5\ 10^{-5}$	$(dm^3)^2/mol/g/min$	33.4
K_{Ac}/K_F	$0.7\ 10^{-2}$	dm^3/mol	7
K_{FAc}/K_F	$0.3\ 10^{-6}$	dm^3/mol	> 1000
K_{F2AcOH}/K_F	3.26	dm^3/mol	22.7
K_{F2Ac}/K_F	0.8	dm^3/mol	16.3
K_{FOh}/K_F	4.1	dm^3/mol	40.1
k_d	$0.3\ 10^{-2}$	$dm^3/g/min^{2.3}$	57.4
k_{df}	1.27	-	34.2
n	2.3	-	7.2
a_∞	0.02	-	17.2
E_{act1}	20.4	kJ/mol	5.4
E_{act2}	29.4	kJ/mol	4.9
E_{act4A}	n.d.	kJ/mol	> 1000
E_{act4B}	4.2	kJ/mol	> 100
E_{act5}	81	kJ/mol	22.1

comprises two terms with the first one reflecting residual activity at infinite time and the second depending on time, catalyst bulk density and the molar ratio of furfural and acetone:

$$a = a_\infty + a\left(t, \rho_B, c_{furfural}/c_{acetone}\right) \tag{12}$$

or more specifically:

$$a = a_\infty + \frac{1}{1 + k_d \rho_B t^n e^{-k_{df}\frac{c_{furfural}}{c_{acetone}}}} \tag{13}$$

In Eq. (13) n, k_d and k_{df} are constants determined through numerical data fitting. Two separate terms for deactivation were introduced to account for the presence of residual activity a_∞ at infinite time. The other term reflects steepness of catalyst deactivation. Time dependent catalyst deactivation is typically expresed by the exponential decay functions, which was not operative in the current case.

An alternative is to consider a deactivation function of the type $a = a_\infty + 1/(1 + k' t^n)$ which exhibits a reciprocal dependence on the reaction time to a certain power. In the current case as deactivation behavior was seen to be dependent on the catalyst loading and the ratio between the reactants, these parameters have been also introduced in Eq. (13).

Apparently more mechanistically sound models for catalyst

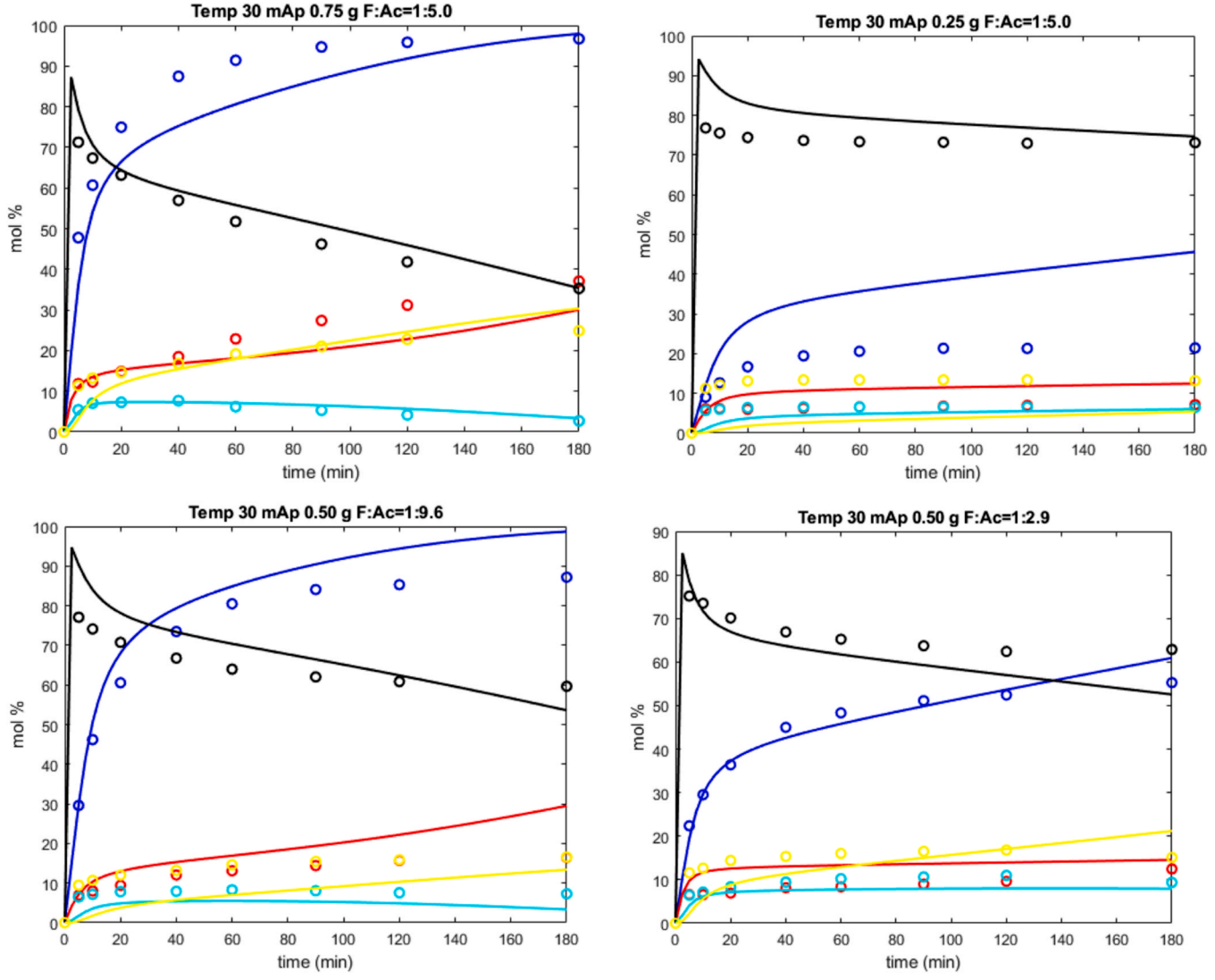

Fig. 12. Comparison between experimental (points) and calculated values (lines) for all experiments. Conversion (blue), selectivity to FAcOH (black), FAc (red), F2AcOH (cyan) and F2Ac (yellow).

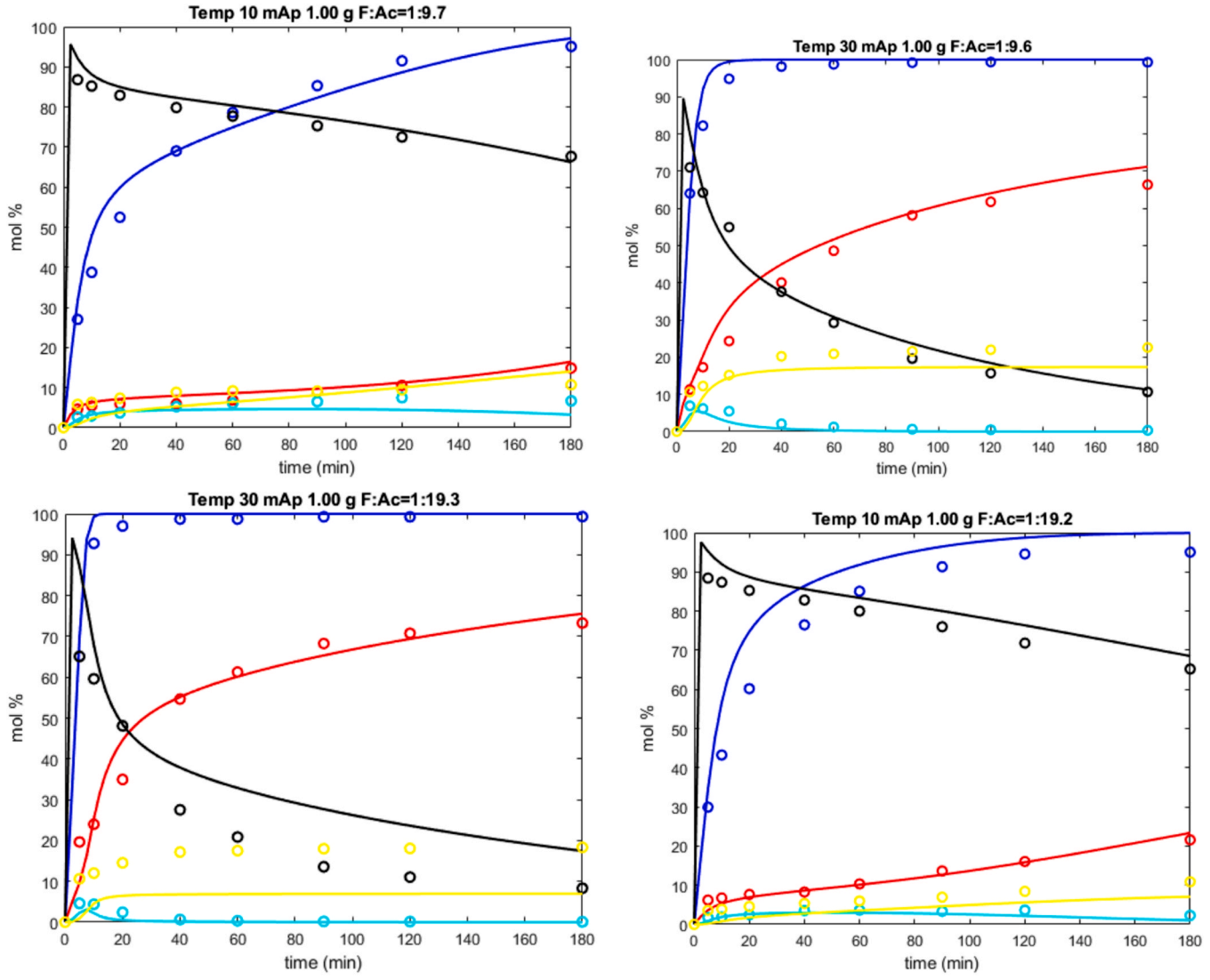

Fig. 12. (*continued*).

inactivation should include not the reaction time but rather conversion and product concentrations being more closely associated with the intrinsic reaction and deactivation mechanisms.

Preliminary calculations indicated that the adsorption terms are significant compared to unity, thus Eqs. (8) and (9) can be modified, giving first

$$D' = c_F + K_{Ac}\quad c_{Ac}/K_F + K_{FAC}\quad c_{FAc}/K_F + K_{F2AcOH}\quad c_{F2AcOH}/K_F + K_{F2Ac}\quad c_{F2Ac}/K_F + K_{FOH}\quad c_{FOH}/K_F \tag{14}$$

and then in combination with Eq. (8).

$$\begin{aligned} r_1 &= \frac{k_1 c_F c_{Ac}}{(K_F D')^2}; \\ r_2 &= \frac{k_2\quad c_{FAcOH}}{K_F D'}; \\ r_{4A} &= k_{4A}\frac{c_{FAc} c_F}{(K_F D')^2}; \\ r_{4B} &= k_{4B}\frac{c_{F2AcOH}}{K_F D'}; \\ r_5 &= k_5 c_F^2; \\ r_6 &= k_6 c_{FCOOH} \end{aligned} \tag{15}$$

The coefficient of determination R^2, which compares the model performance with respect to the variance of all experimental points, was equal to 97.05%. The values of parameters with the respective errors are presented in Table 3, while comparison between the experimental and calculated values is given in Fig. 12. It follows from Table 3 that apparently acetone and FAc are adsorbed weaker than furfural, which F2AcOH, F2AC and furfuryl alcohol have apparently similar values of adsorption constants. The values of activation energies for the aldol condensation reactions are rather while at the same time furfural disproportionation has a much higher energy. An analysis of the activation energy is, however, not straightforward also considering specific features of the hydrotalcite catalyst and its sensitivity to the water content.

The calculated kinetic curves demonstrated in Fig. 12 illustrate overall a good description of the experimental data at different temperatures, concentrations of reactants, and the catalyst mass, which apparently influenced the catalyst deactivation. Just three parameters were not statistically sound, which is acceptable considering a relatively large number of parameters.

Some deviations in the description of the data are visible from Fig. 12 mainly related to concentration of F2Ac, i.e. the ultimate reaction product, and in some cases also related to the conversion of furfural.

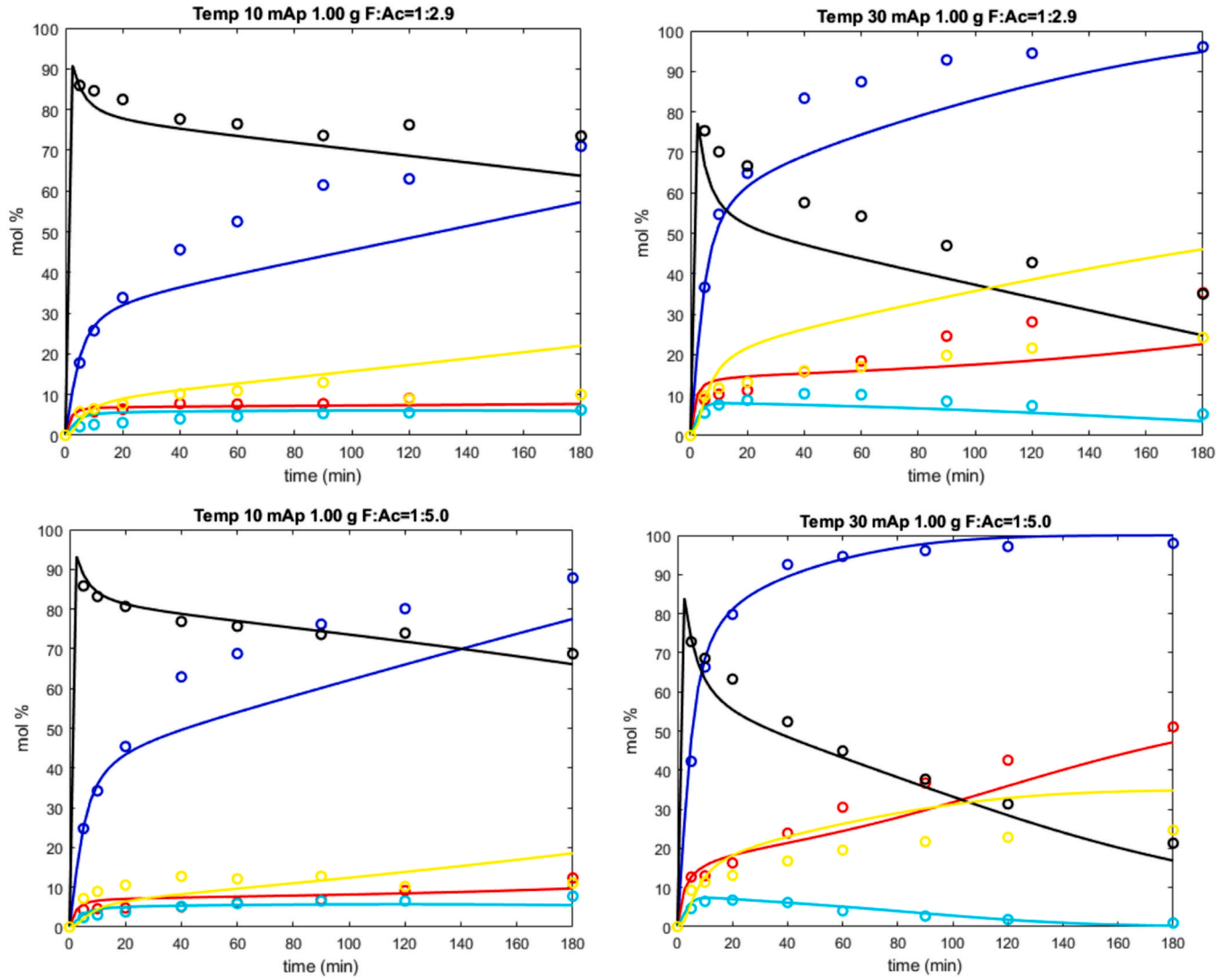

Fig. 12. (*continued*).

4. Conclusions

In this study, the effect of reaction variables on the performance of rehydrated MgAl hydrotalcite in aldol condensation of furfural and acetone was investigated in detail leading to development of the reaction network and kinetic modelling based on this network. The experiments demonstrated that an increase in reaction temperature, catalyst loading, or the amount of acetone in the reaction mixture resulted in an increase in the initial rate of furfural consumption and, as a result, an increase in the final furfural conversion after 180 min of the reaction. The obtained experimental data, as well as the calculations of the Gibbs free energy for each individual chemical reaction in the network suggested that the reaction thermodynamics was favorable for the aldol condensation. Experiments at low reaction temperature or with decreased catalyst loading evidenced elevation of catalyst deactivation that occurred at low furfural consumption rate. Such deactivation allowed suggesting that, at high furfural concentration in the reaction mixture, two parallel processes took place: i) aldol condensation of furfural and acetone and ii) the Cannizzaro reaction with the formation of furfuryl alcohol and furoic acid. Comparing selectivity vs conversion profiles demonstrated that the rates of individual chemical reactions had different activation energies. A change in the selectivity profiles obtained in experiments with different catalyst loadings indicated that the catalyst deactivation was more likely influencing the first step of aldol condensation, i.e. FAc-OH formation, rather than its subsequent dehydration to FAc.

Kinetic modelling described both a change in the concentration of reactants and deactivation of the catalyst surface with carbon deposits was performed based on the proposed reaction network. The calculated kinetic curves showed a good agreement with the obtained experimental data and proved that the change in reaction variables, i.e. reaction temperature, the concentration of reactants, and the catalyst loading had a big impact on both the reaction rate and catalyst deactivation. The results obtained in this study can be further used to optimize conditions to perform aldol condensation of furfural and acetone in presence of heterogeneous basic catalysts.

CRediT authorship contribution statement

Valeriia Korolova: Investigation, Writing first draft. **Oleg Kikhtyanin:** Supervision, Writing – review & editing. **Evgeniya Grechman:** Investigation. **Vincenzo Russo:** Investigation. **Johan Wärnå:** Investigation. **Dmitry Yu. Murzin:** Supervision, Writing - review & editing. **David Kubička:** Supervision, Writing – review & editing.

Declaration of Competing Interest

The authors declare that they have no known competing financial

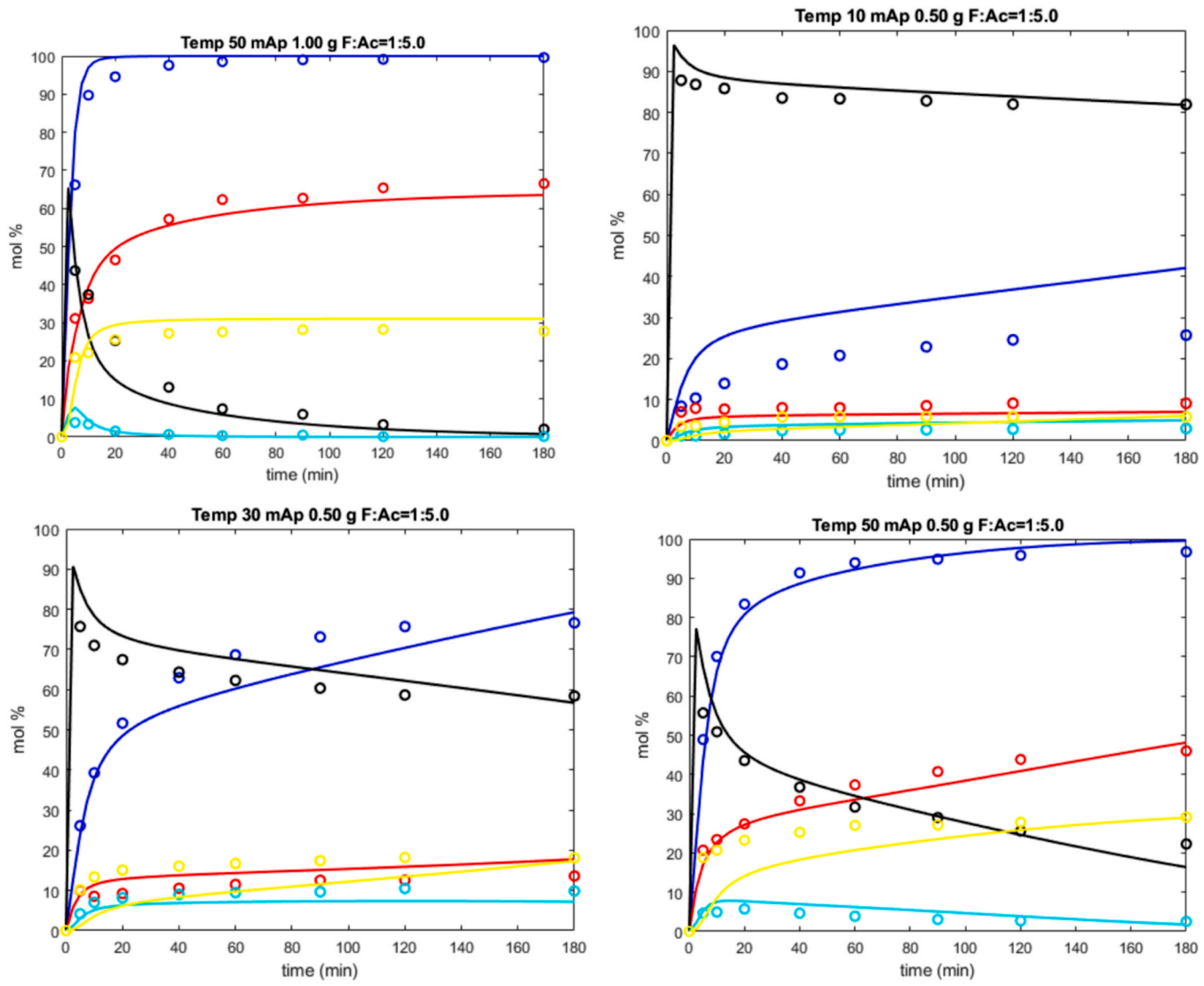

Fig. 12. (*continued*).

interests or personal relationships that could have appeared to influence the work reported in this paper.

Data Availability

Data will be made available on request.

Acknowledgements

The experimental work was supported from the grant of Specific university research – grant No. A1_FTOP_2023_005.

References

[1] D.M. Alonso, J.Q. Bond, J.A. Dumesic, Green. Chem. 12 (2010) 1493–1513.
[2] A. Corma, S. Iborra, A. Velty, Chem. Rev. 107 (2007) 2411–2502.
[3] J. Cueto, L. Faba, E. Díaz, S. Ordonez, Appl. Catal. B: Environ. 201 (2017) 221–231.
[4] M. Su, W. Li, Q. Ma, B. Zhu, J. Bioresources, Bioprod 5 (2020) 256–265.
[5] A. Bohre, S. Dutta, B. Saha, M.M. Abu-Omar, ACS Sustain. Chem. Eng. 3 (2015) 1263–1277.
[6] L. Hora, V. Kelbichová, O. Kikhtyanin, O. Bortnovskiy, D. Kubička, Catal. Today 223 (2014) 138–147.
[7] C.J. Barrett, J.N. Chheda, G.W. Huber, J.A. Dumesic, Appl. Catal. B: Environ. 66 (2006) 111–118.
[8] V.K. Díez, C.R. Apesteguía, J.I. Di Cosimo, J. Catal. 240 (2006) 235–244.
[9] J. Yang, S.S. Li, L. Zhang, X. Liu, J. Wang, X. Pan, N. Li, A.Q. Wang, Y. Cong, X. D. Wang, T. Zhang, ChemSusChem 6 (2013) 1149–1152.
[10] D. Nguyen Thanh, O. Kikhtyanin, R. Ramos, M. Kothari, P. Ulbrich, T. Munshi, D. Kubička, Catal. Today 277 (2016) 97–107.
[11] L. Faba, E. Díaz, S. Ordónez, Appl. Catal. B: Environ. 113–114 (2012) 201–211.
[12] O. Kikhtyanin, R. Bulánek, K. Frolich, J. Cejka, D. Kubicka, J. Molec. Catal. A: Chem. 424 (2016) 358–368.
[13] O. Kikhtyanin, Y. Ganjkhanlou, D. Kubička, R. Bulánek, J. Čejka, Appl. Catal. A: Gen. 549 (2018) 8–18.
[14] H. Naka, Y. Kaneda, T. Kurata, J. Oleo Sci. 50 (2001) 813–821.
[15] O. Kikhtyanin, V. Kelbichová, D. Vitvarová, M. Kubů, D. Kubicka, Catal. Today 227 (2014) 154–162.
[16] A. Dhakshinamoorthy, M. Opanasenko, J. Čejka, H. Garcia, Catal. Sci. Technol. 3 (2013) 5209–5240.
[17] O. Kikhtyanin, D. Kubická, J. Čejka, Catal. Today 243 (2015) 158–162.
[18] B.F. Sels, D.E. de Vos, P.A. Jacobs, Catal. Rev. Sci. Eng. 43 (2001) 443–488.
[19] O. Kikhtyanin, Z. Tišler, R. Velvarská, D. Kubička, Appl. Catal. A: Gen. 536 (2017) 85–96.
[20] O. Kikhtyanin, L. Čapek, L. Smoláková, Z. Tišler, D. Kadlec, M. Lhotka, P. Diblíková, D. Kubička, Ind. Eng. Chem. Res. 56 (2017) 13411–13422.
[21] O. Kikhtyanin, V. Korolova, A. Spencer, L. Dubnová, B. Shumeiko, D. Kubička, Catal. Today 367 (2021) 248–257.
[22] V. Korolova, O. Kikhtyanin, M. Veselý, D. Vrtiška, I. Paterová, V. Fíla, L. Čapek, D. Kubička, Catalysts 11 (2021) 992.
[23] V. Korolova, F. Ruiz-Zepeda, M. Lhotka, M. Veselý, O. Kikhtyanin, D. Kubička, Appl. Catal. A: Gen. 632 (2022), 118482.
[24] S. Abelló, F. Medina, D. Tichit, J. Pérez-Ramírez, J.C. Groen, J.E. Sueiras, P. Salagre, Y. Cesteros, Chem. Eur. J. 11 (2005) 728–739.
[25] S. Abelló, F. Medina, D. Tichit, J. Pérez-Ramírez, J.E. Sueiras, P. Salagre, Y. Cesteros, Appl. Catal. B: Environ. 70 (2007) 577–584.

[26] D. Tichit, B. Coq, CatTech 7 (2003) 206–217.
[27] D.P. Debecker, E.M. Gaigneaux, G. Busca, Chem. Eur. J. 15 (2009) 3920–3935.
[28] D. Tichit, D. Lutic, B. Coq, R. Durand, R. Teissier, J. Catal 219 (1) (2003) 167–175.
[29] X. Fang, Z. Wang, W. Song, S. Li, J. Taiwan, Inst. Chem. Eng. 108 (2020) 16–22.
[30] R.E. O'Neill, L. Vanoye, C. De Bellefon, F. Aiouache, Appl. Catal. B: Environ. 144 (2014) 46–56.
[31] D.S. Desai, G.D. Yadav, Ind. Eng. Chem. Res. 58 (2019) 16096–16105.
[32] N. Fakhfakh, P. Cognet, M. Cabassud, Y. Lucchese, M.D. de Los Ríos, Chem. Eng. Process. 47 (2008) 349–362.
[33] C.J. Jiang, L. Cheng, G.L. Cheng, J. Mater. Sci. Chem. Eng. 6 (2018) 65–73.
[34] R.M. West, Z.Y. Liu, M. Peter, C.A. Gärtner, J.A. Dumesic, J. Molec. Catal. A: Chem. 296 (2008) 18–27.
[35] X. Fang, Z. Wang, W. Song, S. Li, J. Taiwan, Inst. Chem. Eng. 108 (2020) 16–22.
[36] O. Kikhtyanin, E. Lesnik, D. Kubička, Appl. Catal. A: Gen. 525 (2016) 215–225.
[37] J.E. Rekoske, M.A. Barteau, Ind. Eng. Chem. Res. 50 (2011) 41–51.
[38] V.K. Díez, C.R. Apesteguía, J.I. Di Cosimo, Stud. Surf. Sci. Catal. 139 (2001) 303–310.
[39] D. Yang, G. Wang, H. Wu, X. Guo, S. Zhang, Z. Li, C. Li, Catal. Today 316 (2018) 122–128.
[40] W. Shen, G.A. Tompsett, K.D. Hammon, R. Xing, F. Dogan, C.P. Grey, W. Curtis, S. M. Conner Jr, G.W.Huber Auerbach, Appl. Catal. A: Gen. 392 (2011) 57–68.
[41] M.G. Álvarez, R.J. Chimentão, F. Figueras, F. Medina, Appl. Clay Sci. 58 (2012) 16–24.
[42] M.W. Zemansky, M.M. Abbott, H.C. Van, Ness. Basic engineering thermodynamics, McGraw-Hill, New York, 1975.
[43] ChemCAD v.8, ⟨www.chemstations.com⟩.
[44] B.E. Poling, J.M. Prausnitz, J.P. O'Connell, The properties of gases and liquids, McGraw-Hill, New York, 2004.
[45] K.G. Joback, A unified approach to physical property estimation using multivariate statistical techniques. Department of Chemical Engineering, Massachusetts Institute of Technology, Cambridge, MA, 1984. S.M. Thesis.
[46] K.G. Joback, R.C. Reid, Chem. Eng. Comm. 57 (1987) 233–243.
[47] H. Haario, ModEst, The optimization software, Profmath, Helsinki, 2001.